QUALITATIVE ANALYSIS OF NONLINEAR GEAR DRIVE VIBRATION CAUSED BY INTERNAL KINEMATIC AND PARAMETRIC EXCITATION

Miroslav Byrtus*

The methodology of modelling and of qualitative analysis of large rotating systems with gear and bearing couplings is presented. The emphasis is laid on the modelling of nonlinear gear and bearing couplings and on their influence on the dynamic system response to the internal kinematic excitation in gearing and to parametric excitation caused by the time-varying meshing stiffness. The aim is to introduce a method of investigation the behaviour of the rotating system influenced by the mentioned excitation and to examine the influence of chosen operational parameters. The methodology of modelling and of qualitative dynamic behaviour analysis is tested on a two-stage gearbox.

Key words : *vibration, gear drive, nonlinear system, parametric excitation, dynamic analysis*

1. Introduction

This contribution is focused on modelling and analysis of nonlinear systems with a particular application on gear drives that are representatives of nonlinear systems with impacts due to the possibility of gear mesh interruption and consequent impacts in gearing. Similar situations can occur in bearings between rolling-elements and inner or outer race. Moreover, the contact forces transmitted by rolling elements are nonlinear depending on their deformations. And secondly, the gear mesh stiffness can be supposed to be time varying because of the change of number of teeth in gear mesh. These nonlinear phenomena, which are investigated for systems with several DOF number in [3], are sources of nonlinear effects in solution of the model. The time responses of such systems are accompanied by bifurcation of solution in dependence on chosen operational parameters. Vibro-impact systems are characterized by period-doubling scenario, when the period number of the time response increases unexpectedly twice for a certain values of operational parameters. This scenario could repeat till the motion becomes chaotic or the motion could be governed by the reverse period-doubling when the number of periods decreases in the system solution. The ratio of the lengths of successive intervals between values of parameters, for which bifurcation occurs, converges to the first Feigenbaum constant [3].

The paper [5] shows the applicability of presented methodology on a real more-stage gear drive and is focused on detailed description of modelling of nonlinear couplings, but the influence of time varying meshing stiffness is neglected. The aim was to detect boundaries of gear mesh interruption using so called maps of constant gear mesh. The methodology

* Ing. M. Byrtus, Ph.D., Department of Mechanics, Faculty of Applied Sciences, University of West Bohemia, Univerzitní 8, 306 14 Plzeň

of modelling is extended here and the influence of time-varying meshing stiffness and of damping in the gear mesh is taken into account.

2. Nonlinear condensed mathematical model of gear drive

Here, a mathematical model representing a general rotating mechanical system which can be suitably disassembled into S subsystems will be derived. After discretization, each subsystem is described in the local generalized coordinate space $\mathbf{q}_s(t) \in \mathbb{R}^{n_s}$ by a system of n_s ordinary differential equations in the matrix form [4]

$$\mathbf{M}_s\,\ddot{\mathbf{q}}_s(t) + (\mathbf{B}_s + \omega_s\,\mathbf{G}_s)\,\dot{\mathbf{q}}_s(t) + \mathbf{K}_s\,\mathbf{q}_s(t) = \mathbf{f}_s^{\mathrm{E}}(t) + \mathbf{f}_s^{\mathrm{B}} + \mathbf{f}_s^{\mathrm{G}}\;, \qquad s = 1,2,\dots,S\;, \qquad (1)$$

where $\mathbf{M}_s$, $\mathbf{B}_s$ and $\mathbf{K}_s$ are symmetrical mass, damping and stiffness matrices of the uncoupled subsystems of order n_s. Let us suppose the subsystem s rotates with constant angular speed ω_s, then the mathematical model of the subsystem is extended by a skew symmetrical matrix of the gyroscopic effects $\mathbf{G}_s$ of the same order as the matrices mentioned above. All matrices are usually created by means of finite element method combined with discrete parameters, which can represent masses of rigid bodies mounted on the subsystem s. External forced excitation is described by vector $\mathbf{f}_s^{\mathrm{E}}(t)$ and vectors $\mathbf{f}_s^{\mathrm{B}}$ and $\mathbf{f}_s^{\mathrm{G}}$ express bearing and gearing coupling forces including appropriate internal excitation forces. All force effects described in vectors above are acting on the subsystem s.

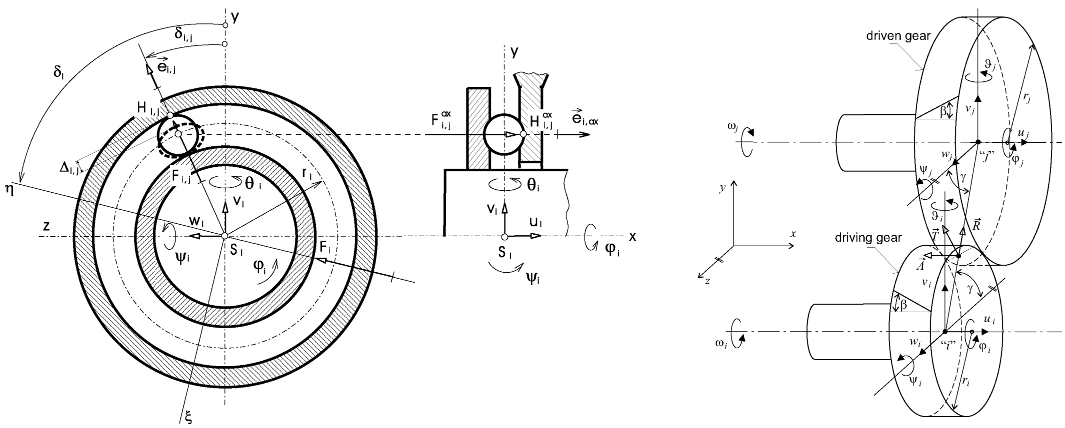

Fig.1: Scheme of bearing and gearing coupling

2.1. Modelling of couplings in gear drives

There are two significant couplings in each gear drive, which are sources of internal excitation and have nonlinear character as well. First, let us focuse on the bearing coupling respecting real number of rolling elements uniform distributed between the inner and outer race (Fig. 1 left). Let us suppose, the rolling-element j of the bearing i touches the outer race at the contact point $H_{i,j}$. Radial (axial) force $F_{i,j}$ ($F_{i,j}^{\mathrm{ax}}$) transmitted at this point depends nonlinearly on the rolling-element deflection $\Delta_{i,j}$ ($\Delta_{i,j}^{\mathrm{ax}}$) according to the Hertz's contact theory, as described in [6]. The calculation of the deflections $\Delta_{i,j}$ supposing the rigid inner and flexible outer race and the possibility of loss of contact between the rolling-element and the race is in detail described in [1].

Then we can define the global bearing coupling vector, which is expressed in the general coordinate space

$$\mathbf{q} = [\,\mathbf{q}_1^{\mathrm{T}} \quad \mathbf{q}_2^{\mathrm{T}} \quad \cdots \quad \mathbf{q}_S^{\mathrm{T}}\,]^{\mathrm{T}} \in \mathbb{R}^n \;, \quad n = \sum_{s=1}^{S} n_s \tag{2}$$

of the whole system in the form [1]

$$\mathbf{f}^{\mathrm{B}} = -\mathbf{K}_{\mathrm{B}}\,\mathbf{q} - \mathbf{B}_{\mathrm{B}}\,\dot{\mathbf{q}} + \sum_{i,j} (\mathbf{c}_{i,j}\,f_{i,j} + \mathbf{c}_{i,j}^{\mathrm{ax}}\,f_{i,j}^{\mathrm{ax}}) \;. \tag{3}$$

where $\mathbf{K}_{\mathrm{B}}$ and $\mathbf{B}_{\mathrm{B}}$ are global stiffness and damping bearing matrices. Their structure depends on the number of rolling elements and on the nodal points to which they are fixed on the shafts (for details see [6]). The damping matrix is supposed to be proportional to the stiffness matrix

$$\mathbf{B}_{\mathrm{B}} = \beta_{\mathrm{B}}\,\mathbf{K}_{\mathrm{B}} \tag{4}$$

and functions $f_{i,j}$ ($f_{i,j}^{\mathrm{ax}}$) take into account nonlinear dependence of rolling-element stiffnesses and the possibility of contact loss for each rolling-element. Vectors $\mathbf{c}_{i,j}$ and $\mathbf{c}_{i,j}^{\mathrm{ax}}$ describe global geometrical properties of contact point j in bearing i.

Secondly, let us deal with the force effect of the spur helical gear coupling G_z, which is expressed in (1) by the vector

$$\mathbf{f}_s^{\mathrm{G}} = \pm \sum_{z} \tilde{\boldsymbol{\delta}}_{z,i}\,F_z(t, d_z, \dot{d}_z) \;, \tag{5}$$

where sign '$-$' (minus) corresponds to driving gear and sign '$+$' (plus) corresponds to driven gear (see Fig. 1 right). The driving (driven) gear is fixed on the shaft at the nodal point i (j). Vector $\tilde{\boldsymbol{\delta}}_{z,i}$ is the n_s-dimensional vector given by extension of the vector $\boldsymbol{\delta}_{z,i}$, whose dimension equals to 6 and describes the basic gearing geometrical parameters. The extension is performed in such a way, when the vector $\boldsymbol{\delta}_{z,i}$ is placed in the vector $\tilde{\boldsymbol{\delta}}_{z,i}$ on the position corresponding to generalized coordinates of the nodal point i. Details are shown in [5]. The resultant force F_z transmitted by gearing G_z considers the gear mesh interruption, the adjustment of backlash in mesh and eventually the influence of time-varying meshing stiffness. The parameter d_z represents the gearing deformation.

Analogous to the bearing model, we can express the global gear coupling vector in the general coordinate space (2) in following way

$$\mathbf{f}^{\mathrm{G}} = -\mathbf{K}_{\mathrm{G}}\,\mathbf{q} - \mathbf{B}_{\mathrm{G}}\,\dot{\mathbf{q}} + \sum_{z=1}^{Z} \mathbf{c}_z\,f_z(t, \mathbf{q}) + \mathbf{f}_{\mathrm{G}}(t) \;, \tag{6}$$

where $\mathbf{K}_{\mathrm{G}}$ and $\mathbf{B}_{\mathrm{G}}$ are global linearized stiffness and damping matrices of gear couplings, whose structure is in detail described in [6]. The function $f_z(t, \mathbf{q})$ corrects the linear elastic part of the gearing force in phases of gear mesh interruption and takes into account the time varying meshing stiffness. The vector $\mathbf{f}_G(t)$ describes internal kinematic excitation generated in gear mesh that can be expressed in the form

$$\mathbf{f}_{\mathrm{G}}(t) = \sum_{z=1}^{Z} \Big(k_z(t)\,\Delta_z(t) + b_z\,\dot{\Delta}_z(t)\Big)\,\mathbf{c}_z \;. \tag{7}$$

The function $\Delta_z(t)$ expresses the kinematic transmission error in gearing G_z and the corresponding global vector of geometrical parameters of the gearing in the general coordinate space (2) is of following structure

$$\mathbf{c}_z = [\cdots \ -\boldsymbol{\delta}_{z,i}^{\mathrm{T}} \ \cdots \ \boldsymbol{\delta}_{z,j}^{\mathrm{T}} \ \cdots \mid \mathbf{0}^{\mathrm{T}}]^{\mathrm{T}} \ , \tag{8}$$

where the meaning of vectors $\boldsymbol{\delta}_{z,i}$ and $\boldsymbol{\delta}_{z,j}$ is given above. Indices i and j correspond to nodal points to which the driving and driven wheels are fixed. And these vectors are placed on positions determined by generalized of coordinates of the nodal points.

The behaviour of the gear coupling is moreover influenced by the periodic time-varying meshing stiffness. The stiffness of a particular gear mesh is considered to be periodic. The period depends on the time duration of one tooth pair mesh. It is influenced by the tooth profile, profile error, gear contact ratio and lubricant properties in gearing.

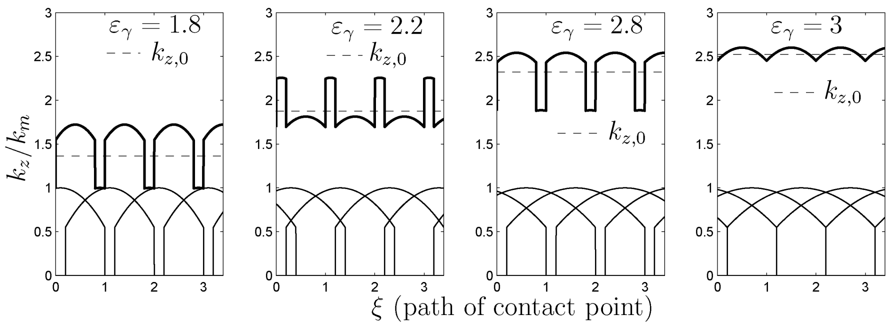

Fig.2: Relative gear mesh stiffness for different values of contact ratio ε_γ

Particular courses of the mesh stiffness can be expressed in a analytical way. Authors [2] proposed the gear mesh stiffness $k_p(t)$ for a single tooth pair p in the form

$$k_p(t) = \begin{cases} k_{\mathrm{m}} \left[-\dfrac{1.8}{(\varepsilon_\gamma T)^2} (t-t_p)^2 + \dfrac{1.8}{\varepsilon_\gamma T} (t-t_p) + 0.55 \right] & \text{for} \quad t \in \{t_p, t_p + \varepsilon_\gamma T\} \ , \\ 0 & \text{otherwise} \end{cases} \tag{9}$$

depending on the contact ratio ε_γ and on the period of the gear mesh T. The parameter k_{m} represents maximum value of the gear mesh stiffness of one tooth pair on the assumption that at time $t = t_p$ teeth enter into mesh and at $t = t_p + \varepsilon_\gamma T$ get out of the mesh. The gear mesh period fulfills

$$T = \frac{2\pi}{p_{\mathrm{z}}\,\omega} \ , \tag{10}$$

where parameter p_{z} indicates the number of the teeth of the driving gear mounted on a shaft rotating with angular velocity ω. The resulting meshing stiffness can be then expressed in following form

$$k_{\mathrm{z}}(t) = \sum_p k_p(t) \ , \tag{11}$$

where index p is restricted to the tooth pairs which are in gear mesh for the given time t. Chosen courses of meshing stiffness are plotted for different contact ratios ε_γ in Fig. 2. The thin lines correspond to meshing stiffness of single tooth pairs and the bold lines display the resulting meshing stiffness influenced by changing of number of tooth pairs being in the mesh.

2.2. Condensed mathematical model of the gear drive

Using the modal transformations

$$\mathbf{q}_s(t) = {}^m\mathbf{V}_s\,\mathbf{x}_s(t)\ , \qquad s = 1, 2, \dots, S\ , \tag{12}$$

defined by modal submatrices ${}^m\mathbf{V}_s \in \mathbb{R}^{n_s,m_s}$ obtained from modal analysis of the mutually uncoupled, undamped and non-rotating subsystems, whereas m_s ($m_s \le n_s$) is the number of the chosen master modes of vibration, we can introduce the new configuration space of the dimension m by the vector

$$\mathbf{x} = [\,\mathbf{x}_1^{\mathrm{T}} \quad \cdots \quad \mathbf{x}_2^{\mathrm{T}} \quad \cdots \quad \mathbf{x}_S^{\mathrm{T}}\,]^{\mathrm{T}}\ , \qquad m = \sum_{s=1}^{S} m_s\ . \tag{13}$$

The model (1) can be then rewritten using terms (3) and (6) in the global condensed form

$$\ddot{\mathbf{x}}(t) + \Big[\mathbf{B} + \omega_0\,\mathbf{G} + \mathbf{V}^{\mathrm{T}}\,(\mathbf{B}_{\mathrm{B}} + \mathbf{B}_{\mathrm{G}})\,\mathbf{V}\Big]\dot{\mathbf{x}}(t) + \Big[\mathbf{\Lambda} + \mathbf{V}^{\mathrm{T}}\,(\mathbf{K}_{\mathrm{B}} + \mathbf{K}_{\mathrm{G}})\,\mathbf{V}\Big]\mathbf{x}(t) =$$
$$= \mathbf{V}^{\mathrm{T}}\Big[\sum_i\sum_j\big(\mathbf{c}_{i,j}\,f_{i,j}(\mathbf{q}) + \mathbf{c}_{i,j}^{\mathrm{ax}}\,f_{i,j}^{\mathrm{ax}}(\mathbf{q})\big) + \sum_{z=1}^{Z}\mathbf{c}_z\,f_z(t,\mathbf{q}) + \mathbf{f}_{\mathrm{G}}(t) + \mathbf{f}_{\mathrm{E}}(t)\Big]\ , \tag{14}$$

where $\mathbf{f}_{\mathrm{E}}(t) = [\,(\mathbf{f}_1^E(t))^{\mathrm{T}},\ (\mathbf{f}_2^E(t))^{\mathrm{T}},\ \cdots\ ,\ (\mathbf{f}_S^E(t))^{\mathrm{T}}\,]^{\mathrm{T}}$ is the global vector of external excitation,

$$\mathbf{B} = \mathrm{diag}\left({}^m\mathbf{V}_s^{\mathrm{T}}\,\mathbf{B}_s{}^m\,\mathbf{V}_s\right)\ ,\quad \mathbf{G} = \mathrm{diag}\left(\frac{\omega_s}{\omega_0}\,{}^m\mathbf{V}_s^{\mathrm{T}}\,\mathbf{G}_s{}^m\,\mathbf{V}_s\right)\ ,\quad \mathbf{V} = \mathrm{diag}\left({}^m\mathbf{V}_s\right) \tag{15}$$

are block diagonal matrices ($\omega_S = 0$ holds for the stator subsystem) and $\mathbf{\Lambda} = \mathrm{diag}\,({}^m\mathbf{\Lambda}_s)$ is diagonal matrix composed of spectral submatrices ${}^m\mathbf{\Lambda}_s \in \mathbb{R}^{m_s,m_s}$ of the subsystems.

3. Analysis of two-stage gearbox nonlinear vibration

This chapter presents an application of the above mentioned methodology of mathematical modelling of large rotating systems and shows some ways how to analyze the dynamic behaviour of this class of mechanical systems.

3.1. Description of the model

The presented methodology of modelling was applied to a two-stage test gearbox (Fig. 3). The gearbox can be decomposed into three subsystems – driving shaft with gears ($s = 1$), driven shaft with gears ($s = 2$) and the housing ($s = 3$) wired in several nodal points with the fixed frame. Subsystems are joined by discrete couplings – gear meshes (G_1 and G_2) and rolling-element bearings (B_1 to B_4) considering twenty rolling-elements. The initial number of DOF of the uncoupled subsystems after discretization by FEM was $n_1 = 91$, $n_2 = 92$ (driving and driven shaft) and $n_3 \sim 15000$ (housing) using MATLAB code for rotating subsystems and software package ANSYS for the housing. Numerical experiments show that the reduced (condensed) model (14) of the complete system of the order $m = 160$ ($m_1 = m_2 = 30$, $m_3 = 100$) is acceptable in the frequency range up to 5000 Hz.

The main source of excitation is the internal transmission error in the gear mesh G_1 transmitting the power in the gearbox. It was approached by the Fourier series taking into account only first three amplitudes (7) of values $\Delta_{1,1} = 5\,\mu$m, $\Delta_{1,2} = 2.5\,\mu$m and $\Delta_{1,3} = 1.66\,\mu$m. The second gear mesh G_2 does not transmit the power and includes one gear fixed on the driving shaft and one gear which can freely rotate around the driven shaft. The mathematical model of the gear drive is then strongly nonlinear due to the possibility of gear mesh interruption in both gear meshes and in consequence of nonlinear bearing couplings respecting loss of contact in some contact points in dependence on position of journal centre. The stiffness of each rolling element is a nonlinear function of its deformation. To perform the dynamic analysis the condensed mathematical model (14) has to be transformed into the state space to use the time integration method started from initial state defined by

$$\mathbf{x}(0) = [\mathbf{\Lambda} + \mathbf{V}^{\mathrm{T}}(\mathbf{K}_{\mathrm{B}} + \mathbf{K}_{\mathrm{G}})\,\mathbf{V}]^{-1}\,\mathbf{V}^{\mathrm{T}}\,\mathbf{f}_{\mathrm{E}}(0)\ , \qquad \dot{\mathbf{x}}(0) = \boldsymbol{\omega}_0 \tag{16}$$

to minimize the startup transient motions. In general, the vector $\mathbf{f}_{\mathrm{E}}(0)$ can describe an arbitrary external excitation at the start of numerical integration and the vector $\boldsymbol{\omega}_0$ defines angular velocity in each nodal point in dependence on angular velocity of the driving shaft. In this case, the vector $\mathbf{f}_{\mathrm{E}}(0)$ expresses the external static load defined by the static deformation of the torsion couplings $\Delta\varphi = \Delta\varphi_1 = \Delta\varphi_2$ (see Fig. 3).

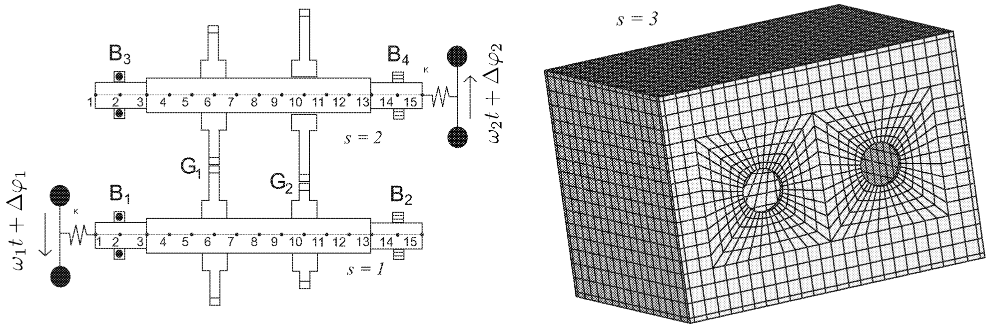

Fig.3: Scheme of two-stage test gearbox

3.2. Dynamic analysis

Here, we are concerned with the qualitative analysis of the behaviour of the two-stage test gearbox vibration. The motion of the gearbox is mostly influenced by the transmission error in gearing G_1 transmitting the power, which can cause not only the interruption of gear mesh G_1 but it can also influence the motion of the freely rotating gear in gear mesh G_2. The next internal excitation source is the time dependent change of the meshing stiffness, which we suppose in the gear mesh G_1 only. The final behaviour of the complete system depends then on operational parameters, which were chosen in following way: revolution of the driving shaft and the static load (power) transmitted by the rotating parts that is described by the deformation $\Delta\varphi$.

The nonlinear behaviour of the system is displayed using bifurcation diagrams, where the maxima (gray) and minima (black) of gearing deformation (GD) are plotted on the vertical axis. Numerical simulations have shown the direct dependence between the character of behaviour of the system and the character of GD. The change of the chosen operational parameter is plotted on the horizontal axis. This representation of results is illustrative for detection of gear mesh interruption, bifurcation of solution and chaotic motion.

Fig. 4 displays the bifurcation diagram of GD in dependence on revolutions per minute of the driving shaft for static load defined by $\Delta\varphi = 0.03\,\mathrm{rad}$. Negative values of GD correspond to gear mesh interruption. The backlashes of both meshes have a value of $12\,\mu\mathrm{m}$. The

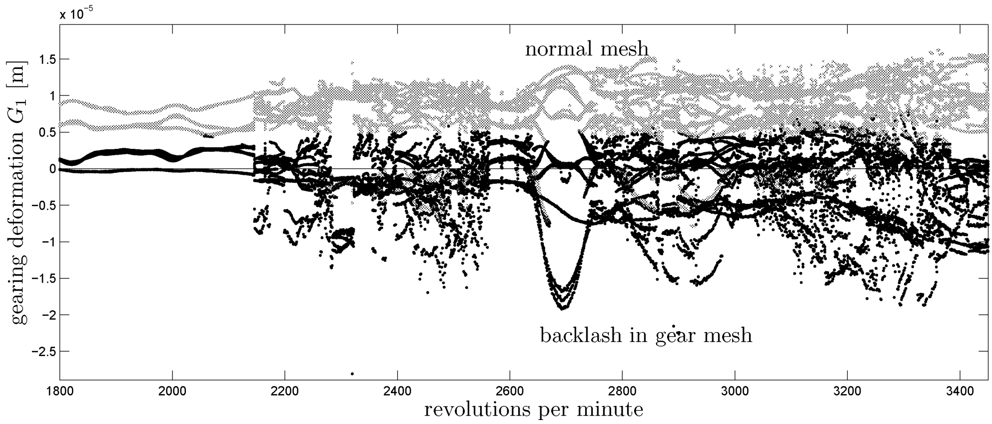

Fig.4: Bifurcation diagram of gearing deformation in dependence on revolutions of driving shaft under assumption of constant meshing stiffness

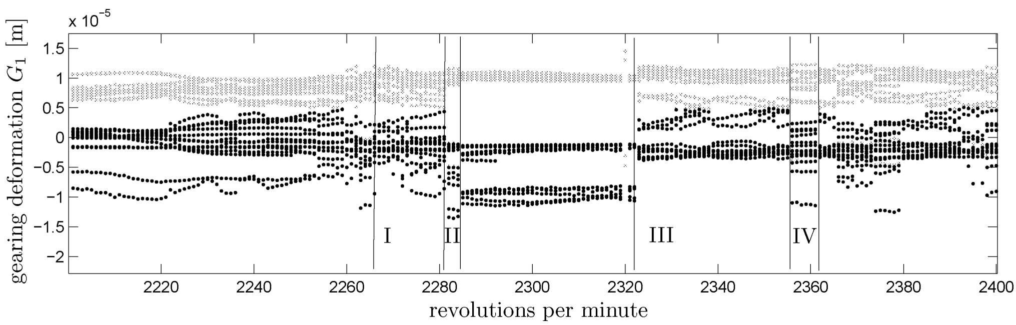

Fig.5: Detection of period-doubling scenario

diagram shows the structure of behaviour of the gearing and consequently of the whole system. The solution is accompanied by gear mesh interruptions in the whole operational area and by transitions among solutions and their bifurcation.

If we zoom a chosen area of the bifurcation diagram in the range from 2200 to 2400 rpm, we obtain more transparent view of the character of the system behaviour. On fig. 5 the changes among solutions can be clearly seen, especially the bifurcations of solution. There are designated four areas by I, II, III, IV and borders between them correspond to values of revolutions of the driving shaft, for which the bifurcations occur. We can observe, the characteristic of nonlinear behaviour is determined by the period-doubling scenario, when the ratio of two following length of mentioned areas is approximately equal to first Feigenbaum number $\delta = 4.66292$, especially the ratios of I/II and III/IV.

Fig. 6 shows the evolution of solution character in dependence on external static load of the gear drive. For a small load $\Delta\varphi \in \langle 0.001, 0.022\rangle$ the motion is chaotic and is characterized by impacts and changing of normal and inverse mesh. For $\Delta\varphi \in \langle 0.022, 0.031\rangle$ the motion is still chaotic but the inverse mesh disappeared. Increasing the external load, the motion becomes periodic with impacts till $\Delta\varphi = 0.083$ and then the gear mesh is constant.

Further, the influence of damping coefficient b_1 in gearing G_1 was examined. We have defined the damping ratio b_1/b_1^{ref}, where the parameter b_1^{ref} is a reference damping coefficient of value $b_1^{\mathrm{ref}} = 1.63\times10^3\,\mathrm{kg\,s^{-1}}$. Fig. 7 and Fig. 8 show the character of solution in dependence

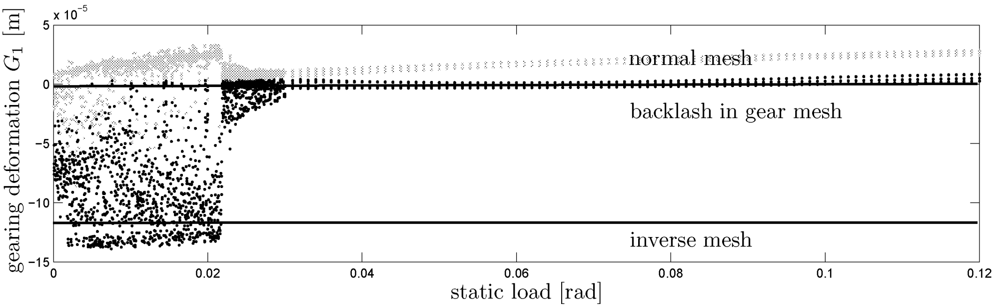

Fig.6: Bifurcation diagram of gearing deformation in dependence on external static load which is represented by static deformation $\Delta\varphi$ under assumption of constant meshing stiffness

on the damping ratio $b_1/b_1^{\rm ref}$. The first figure corresponds to solution gained considering the constant meshing stiffness. The second one is obtained under the assumption of time varying meshing stiffness with no shift between phases of kinematic transmission error in gearing and the varying meshing stiffness. The character of solutions changes by increasing the damping ratio in general. But the difference of solutions according the mentioned assumptions is not significant. The time-varying meshing stiffness does not change the range of maxima and minima of GD, but it influences the character of solution. The areas of periodic or quasi-periodic solutions (for $b_1/b_1^{\rm ref} \in \langle 0.3, 2\rangle$) plotted in Fig. 7 overcame into areas of chaotic solutions (for $b_1/b_1^{\rm ref} \in \langle 0.3, 1.2\rangle$) in Fig. 8.

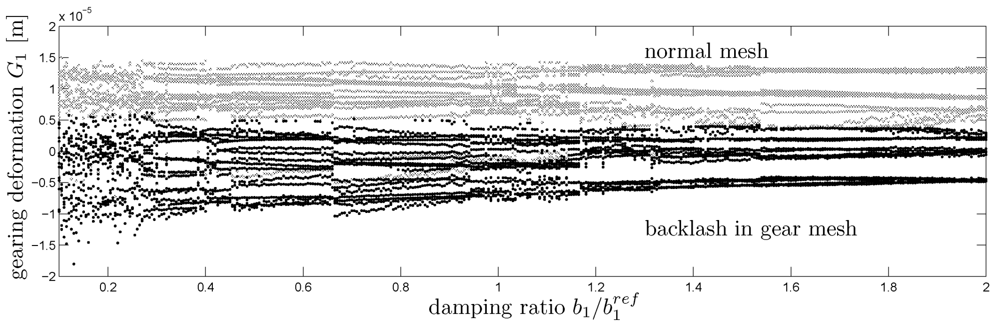

Fig.7: Bifurcation diagram of gearing deformation in dependence on damping ratio $b_1/b_1^{\rm ref}$ of gearing G_1 under assumption of constant meshing stiffness

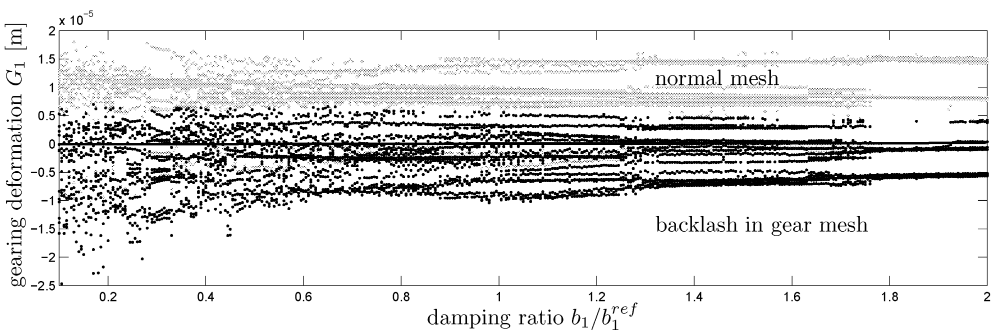

Fig.8: Bifurcation diagram of gearing deformation in dependence on damping ratio $b_1/b_1^{\rm ref}$ of gearing G_1 under assumption of time-varying meshing stiffness

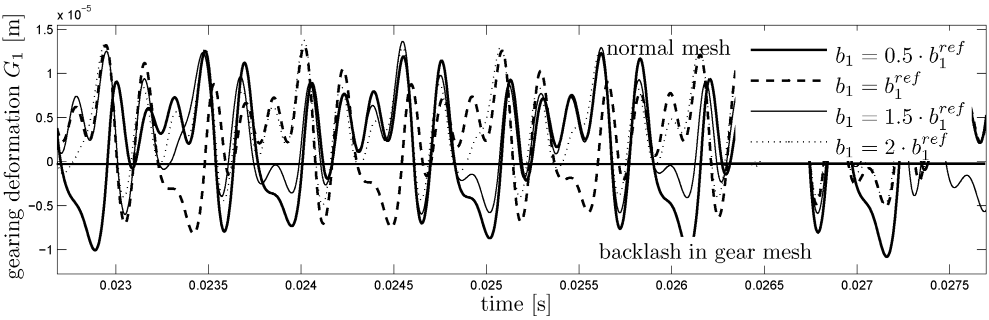

Fig.9: Time course of gearing deformation G_1 for different damping coefficients

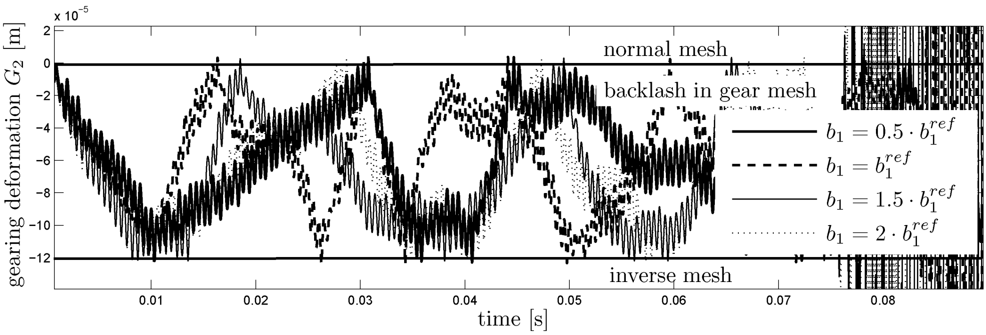

Fig.10: Time course of gearing deformation G_2 for different damping coefficients

Time courses of GD G_1 and G_2 are plotted for four different damping coefficients b_1 in last two figures. The change of damping b_1 causes time shifts and change of shape of gearing deformation in G_1. Moreover, it influences the time points of impacts in G_2 with the freely rotating gear. The impacts appear at the point of normal mesh as well as at the point of inverse mesh. For long time simulation the system becomes unstable (see Fig. 10, $t > 0.076$ s). Probably, it is caused by the unstability of chosen numerical method.

4. Conclusion

The paper describes the methodology of large coupled rotating systems modelling represented by gear drives. The models of these systems suppose a flexible stator and nonlinear gear couplings between rotor subsystems, nonlinear rolling-element bearings and the parametric excitation in gearing. The model of the whole system is created by means of the modal synthesis method which allows to reduce the degrees of freedom number of the mathematical model. The goal of this contribution was to show the applicability of the methodology on multi-stage gear drives and to perform the dynamic analysis of nonlinear vibrations excited by kinematic transmission error and parametric excitation in gearing accompanied by impacts in gear mesh. According to gained results, the motion of nonlinear model of the gear drive is represented by nonlinear phenomena for certain operational parameters. These kinds of solution are very interesting from the theoretical point of view.

Acknowledgement

This work was supported by the research project MSM 4977751303 of the Ministry of Education, Youth and Sports of the Czech Republic.

References

[1] Byrtus M.,Zeman V.: Modal synthesis method applied to nonlinear systems, In Proc. of Colloquium Dynamics of Machines 2007, pages 21–28, Prague, February 6–7, 2007
[2] Cai Y., Hayashi T.: The linear approximated equation of vibration of a pair of spur gears (Theory and experiment), In Journal of Mechanical Design, 1994, 116, pp. 558–564
[3] Thompson J.M., Stewart H.B.: Nonlinear dynamics and chaos, John Wiley & Sons, Chichester, 2002
[4] Zeman V.: Vibration of Mechanical Systems by the Modal Synthesis Method, In ZAMM – Z. angew. Math. Mech., 1994, 75(4), pp. 99–101
[5] Zeman V., Byrtus M.: Mathematical modelling of nonlinear gearbox vibration, In Proceedings of 12th world congress in mechanism and machine science, June 17-21, 2007, Besançon, France.
[6] Zeman V., Hajžman M.: Modelling of shaft system vibration with gears and rolling element bearings, In Proc. of Colloquium Dynamics of Machines 2005, pages 163-170, Prague, February 8–9, 2005

Received in editor's office: March 25, 2008
Approved for publishing: August 11, 2008